

Unified Kinetic Model for Cellulose Deconstruction via Acid Hydrolysis

G. SriBala[†] and R. Vinu^{†,‡,*}

[†]Department of Chemical Engineering, Indian Institute of Technology Madras, Chennai – 600036, India

[‡]National Center for Combustion Research and Development, Indian Institute of Technology Madras, Chennai – 600036, India

ABSTRACT: Kinetics of cellulose acid hydrolysis is reported to be very different under dilute acid–high temperature and concentrated acid–low temperature conditions due to the heterogeneous and homogeneous nature of the reactions, respectively. This work aims at unifying the kinetics of cellulose deconstruction by developing a mechanistic model that includes formation and decomposition of glucose and cellulo-oligomers under extremely low (0.07%) to high (70%) acid concentrations and high (225 °C) to low (25 °C) temperatures. A continuous distribution kinetic model that includes (i) random mid-chain and specific end-chain scission of cellulose to form cellulo-oligomers and glucose; (ii) specific scission of cellulo-oligomers to form glucose, cellobiose, cellotriose, cellobiose, and cellopentaose; and (iii) degradation of glucose was developed. The model predicted reasonably well the experimental data of concentration of cellulose, glucose, and other oligomers obtained from different studies in a broad range of acid concentrations and temperatures. The effects of initial concentration and degree of polymerization on cellulose conversion and glucose yield were evaluated using this model. Moreover, the model also predicted various reported physical effects on cellulose deconstruction and, importantly, manifested its applicability for cellulose hydrolysis in lignocellulosic biomasses like walnut green skin and yellow poplar wood.

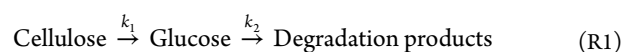
1. INTRODUCTION

Owing to perishing fossil fuel reserves there is a constant thrust to employ alternative energy resources to meet fuel demands. Lignocellulosic biomasses like sugar cane bagasse, corn stover, wheat straw, and hardwood, which are generated as waste byproducts, prove to be some of the potential resources that can fulfill the needs of the energy sector. Although it is a good alternate fuel, the high cost of its production, especially in pretreating the feedstocks, brings down its usage.^{1–3}

Cellulose, a homopolymer of glucose, is one of the major components of lignocellulosic biomass constituting nearly 20–50 wt %, while others include hemicellulose (15–30 wt %), lignin (10–30 wt %), and ash (5–10 wt %) on a dry basis.⁴ Cellulose has a highly crystalline structure due to the high degree of hydrogen bonding existent between the hydroxyl groups and the glycosidic or ring oxygen atoms. A cross-section of lignocellulosic biomass shows a highly complex matrix of cellulose with interchain, intrachain, and intersheet hydrogen bonding and its linkage to hemicellulose and lignin via hydrogen bonding and lignin–carbohydrate complexes.⁴ Hence, to make cellulose and hemicellulose accessible for the hydrolysis process, the biomass feedstocks have to be pretreated.^{1,3,5,6} Acid hydrolysis is one of the oldest pretreatment techniques, and it has been employed since World War II. It is a very interesting process as it serves both as a pretreatment as well as a saccharification process. According to the Consortium for Applied Fundamentals and Innovation (CAFI) studies, dilute acid hydrolysis is one of the most common methods of pretreatment, others being steam explosion, ozonolysis, and fractionation by phosphoric acid. When this method was carried out under optimal pretreatment conditions, the degree of polymerization, hemicellulose content, and acetyl groups of poplar wood were reduced by

significant numbers in comparison with other pretreatment techniques. Moreover, total fixed capital per gallon of ethanol produced was found to be lesser when the pretreatment process was acid hydrolysis compared to the other common methods.⁷ Hence, this technique is very interesting as it serves both for pretreatment as well as saccharification. Dilute acid hydrolysis mainly serves as a pretreatment for enzymatic hydrolysis. It improves biomass porosity by hemicellulose removal but can only be applied to biomasses with low lignin content. On the other hand, concentrated acid hydrolysis serves the purpose of complete hydrolysis of holocelluloses and results in high sugar yields. Importantly, it is applicable to a very wide range of feedstocks unlike dilute acid hydrolysis.⁸ Many studies have been performed to improve and utilize this process for biofuels production.^{1,3,9,10} There were also a few studies on utilizing extremely low acid conditions to address the setbacks of the existing processes using very high acid concentrations.^{11–13}

The understanding of reaction kinetics is very important while developing any process. The first kinetic model for cellulose acid hydrolysis was first developed by Saeman,¹⁴ who assumed the reactions to occur in two stages, which includes the release of glucose from cellulose and formation of glucose degradation products. This simple series reaction R1 was found to be widely applicable to a variety of lignocellulosic biomasses.



Received: February 24, 2014

Revised: April 21, 2014

Accepted: April 28, 2014

Published: April 28, 2014

Table 1. Overview of Kinetic Parameters of Cellulose Acid Hydrolysis Reported in the Literature

substrate	reaction conditions ^a	k_{10} (min ⁻¹)	E_{a1} (kJ/mol)	m_1	k_{20} (min ⁻¹)	E_{a2} (kJ/mol)	m_2	ref
cellulose pulp from sugar cane bagasse	acid: 0.07–0.28 wt % temp.: 180–230 °C	1.3×10^{19}	184.9		3×10^{12}	124.5		13
douglas fir	acid: 0.4–1.0 wt % temp.: 170–190 °C	1.73×10^{19}	179.5	1.34	2.38×10^{14}	137.5	1.02	14
microcrystalline cellulose	acid: 30–70 wt % temp.: 25–40 °C	2.946×10^{10}	127.2	6.0	7.98×10^{26}	166.9	0.77	16
paper refuse	acid: 0.2–1.0 wt % temp.: 180–240 °C	28×10^{19}	188.7	1.78	4.9×10^{14}	137.2	0.55	17
municipal solid wastes	acid: 1.3–4.4 wt % temp.: 200–240 °C	1.94×10^{16}	171.61	1.0	1.148×10^{12}	142.3	0.66	18
α -cellulose	acid: 0.2–1.0 wt % temp.: 220–240 °C	1.2×10^{19}	177.6	1.3	3.8×10^{14}	136.7	0.7	19
solka-floc	acid: 0.5–2.0 wt % temp.: 180–240 °C	1.22×10^{19}	177.8	1.16	3.79×10^{14}	136.8	0.69	20
filter paper	acid: 0.4–1.5 wt % temp.: 200–240 °C	1.22×10^{19}	178.9	1.16	3.79×10^{14}	137.2	0.69	21
hardwood	acid: 4.41–12.2 wt % temp.: 170–190 °C	6.6×10^{16}	165.34	1.64	6.4×10^{12}	128.9	1.10	22

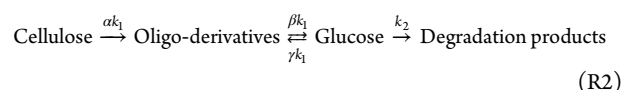
^aAcid used in all the experiments was H₂SO₄. The kinetic parameters correspond to reaction R1 and eq 1.

The above reactions were considered as pseudo-first-order ones by accounting for the acid-dependence term as a parameter of rate constant as shown in the following Arrhenius equation.

$$k_i = k_{i0} A^{m_i} \exp\left(\frac{-E_{ai}}{RT}\right) \quad i = 1, 2 \quad (1)$$

In the above equation, k_{i0} is the pre-exponential factor in time⁻¹, A is the acid concentration, E_{ai} is activation energy in kJ/mol, T is temperature in K, R is the universal gas constant, and m_1 and m_2 are the slopes of cellulose and glucose hydrolysis profiles, respectively. This model was widely used for the kinetic study of the hydrolysis of all types of biomass feedstocks.^{13,15–18} Table 1^{13,14,16–22} lists the values of k_{10} , k_{20} , E_{a1} , E_{a2} , and m_1 and m_2 observed for acid hydrolysis of cellulose extracted from different literature sources at different acid concentrations and temperatures. It is clear that the pre-exponential factors, activation energies, and acid exponents for cellulose hydrolysis to glucose vary in a very broad range, 10^{10} to 10^{19} min⁻¹, 127–188 kJ/mol, and 1.0–6.0, respectively. This indicates that a simple model of hydrolysis cannot be used on the entire range of temperatures and acid concentrations.

Due to the advancements in the analysis techniques, the presence of cellulose-oligomers was discovered, and consequently, the primitive Saeman model had to be modified. Abatzoglov et al.¹⁹ observed the presence of oligo-derivatives in the hydrolysate obtained from α -cellulose. The oligomers were assumed to be intermediate products during the conversion of cellulose to glucose. It was found that the rate of formation of glucose from oligomers is 3 times faster than the formation of the latter from cellulose. Hence the simple series reaction model of Saeman¹⁴ was extended to account for the formation of oligomers in the early stages of hydrolysis according to the following reaction sequence.



The values of α , β , and γ were evaluated to be 0.6, 0.9, and 0.0, respectively. Various other complex kinetic models were proposed, indicating the formation of a nondegradable

oligomer fraction, degradable oligomers that eventually gave rise to monomer sugars, and their degradation products.^{12,23,24} Nevertheless, the Saeman model still stands to be in agreement with various acid hydrolysis experiments.

Although many of the existing models explain the formation of oligomers, however, the lumping of many intermediate reactions limits the applicability of a mechanism for the explanation of the phenomenon of acid hydrolysis, especially when one has to distinguish the exact kinetics of hydrolysis under conventional thermal conditions to that of nonconventional conditions. From the work of Xiang et al.,²⁵ it is evident that the negative slope of glucose degradation profiles decreases with a decrease in pH. Between 7 and 2 pH the slope is nearly the same; however, it changes significantly with even a slight dip in pH below 2. The Saeman model fails to predict such trends. Another limitation of the existing works lies in the choice of the rate parameters at the desired temperature and acid concentration. The rate parameters, namely, activation energy and pre-exponential factor, reported for hydrolysis of cellulose from different sources and at acid concentrations ranging between 0.07 and 70 wt % of acid and 25–240 °C temperature do not fall under a comparable range (Table 1), and hence, it becomes ambiguous to choose a set of values for the desired reaction conditions. Fitting all parameters time and again is quite a tedious job, and this also makes the model invalid for utilization in process modeling suites.

The presented work aims at understanding the kinetics of acid hydrolysis by considering the formation of various low molecular weight products (LMWPs, with degree of polymerization, DP = 1–6) which were observed in significant amounts in the hydrolysate reported by Xiang et al.¹² The key focus of the work is to develop a unified kinetic model for cellulose deconstruction via acid hydrolysis which is applicable for a wide range of acid concentrations and temperatures. The rate parameters, viz. activation energies and pre-exponential factors of all the elementary reactions, were utilized from the literature while a few of the rate controlling parameters such as the exponents of acid concentration and temperature were fitted for different reaction conditions to match the experimental data. In this work, the sensitivity of glucose degradation kinetics

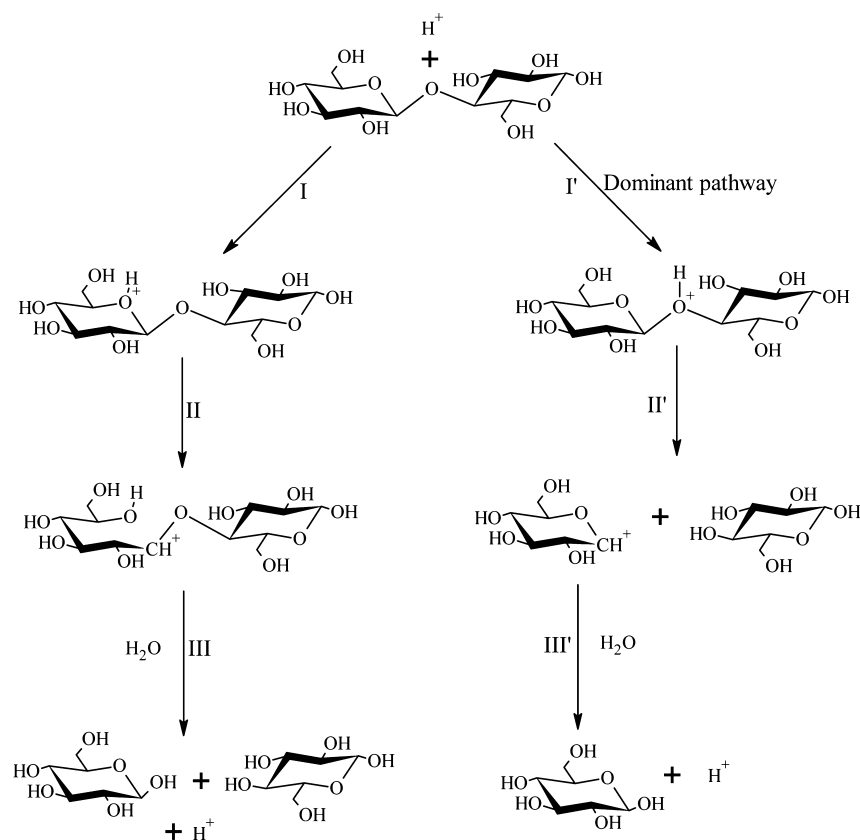


Figure 1. Mechanism of acid hydrolysis of cellobiose.²⁶ I', II', and III' represent three stages of intermediate reactions that take place to release glucose. Similar reactions do occur in the case of cellulose.

with temperature was incorporated by the use of the modified Arrhenius equation, namely with the additional temperature dependent term. Additionally, the versatility of the model was also tested by validating it for the hydrolysis of whole biomasses like walnut green skin and yellow poplar wood.

2. MODEL DEVELOPMENT

2.1. Mechanism of Acid Hydrolysis of Cellulose. Acid hydrolysis of cellulose occurs by disruption of intra- and intermolecular hydrogen bonds with the attack of an acid proton either at glycosidic oxygen or ring oxygen, resulting in a cyclic or a noncyclic carbonium cation, respectively. Thus, the mechanism has two pathways, one of glycosidic bond cleavage and the other by the cleavage at the ring oxygen. The mechanism of proton attack on a cellobiose molecule is depicted in Figure 1. In the dominant pathway (I', II', III') the reaction is initiated by the attack of a proton on the glycosidic oxygen atom, thus forming a conjugate acid. It is propagated by the cleavage of a glycosidic C–O bond giving rise to an intermediate cyclic carbonium cation and an end chain product, i.e. glucose in the depicted case. Further, by the addition of a water molecule to the carbonium cation, the reaction terminates, giving rise to a saccharide and a proton. In the alternate pathway, a proton attacks the ring oxygen resulting in ring-opening and formation of a noncyclic carbonium cation which liberates an acid proton with the addition of water, thereby producing two glucose units. This was proved to be a minor pathway owing to a larger degree of steric effects surrounding the ring oxygen.²⁶ Thus, the acid merely acts as a catalyst in converting polysaccharides to sugars. Moreover, the derived sugars may further decompose due to oxidation of the

reducing end groups. When the acid medium is H₂SO₄, these decomposition products may react with sulfate ions produced by dissociation of H₂SO₄ molecules, giving rise to various acids.²⁶

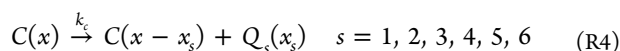
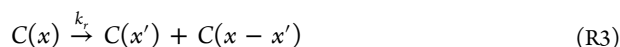
The decomposition of sugars can be controlled by varying the acid concentration. Temperature and pressure are two other parameters that enhance the yield of sugars. Elevated pressures increase the rate of hydrolysis.²⁶ However, at temperatures greater than 30 °C, glucose decomposition reactions are initiated.¹⁶ Acid hydrolysis of lignocellulosic biomass, particularly cellulose, is usually carried out at high acid concentrations and low temperatures or dilute acid concentrations and high temperatures. Although the key reactions are the same in both the reaction regimes, kinetics of hydrolysis remains different due to differences in physical effects occurring at such extreme conditions. Acid hydrolysis under concentrated acid and low temperatures is homogeneous while that at dilute acid and high temperatures is heterogeneous in nature due to varied solvability of cellulose chains by the acidic protons in both cases.²⁷

It was hypothesized that under dilute acid conditions, hydrolysis occurs predominantly at amorphous sites or at the crystal surface. Due to the dense network of intermolecular and interchain hydrogen bonding, the reaction was assumed to occur only at the ends of cellulose chains as the inner glycosidic oxygen atoms remain inaccessible to acid proton attack. Thus, heterogeneous acid attack was considered to cause end-chain scission of cellulose. This was later revised after it was found that the hydrated protons may move through the cellulose crystal lattice. Although there exists a large resistance for the formation of a cyclic carbonium cation due to steric effects

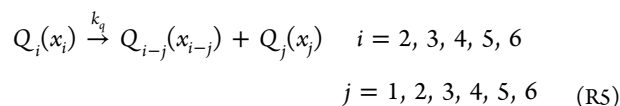
caused by intermolecular hydrogen bonding,²⁷ the possibility of mid-chain scission of the cellulose chain at any random position cannot be completely abandoned.

Another study reported that the orientation of the C6 group determines the fate of the proton attack on the glycosidic oxygen adjacent to its ring. When the C6 group forms a bifurcated hydrogen bond with the hydroxyl group attached to the C3 atom of the ring, it creates a hydrophobic environment around the adjacent glycosidic linkage. Thus, the angle of accessibility of glycosidic oxygen for proton attack is very narrow and resistance to hydrolysis develops. If the orientation of the C6 group allows it to rotate freely, the transfer of a proton to the glycosidic oxygen is favored. Moreover, the bond lengths of the linkages vary due to differences in orientation of bonding orbitals and lone pair orbitals of the oxygen atom. The orientation of the lone pair orbital is effected by the position of the ring oxygen. Thus, the differences in electronic character of the glycosidic linkages affect the proton attack and, in turn, the rates of hydrolysis of the respective glycosidic bonds.²⁸ Therefore, in this work, two types of cellulose chain scission are considered separately to study the kinetics of time evolution of sugars.

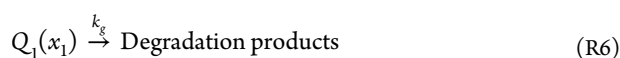
2.2. Rate Equations. Continuous distribution kinetics was adopted to model the reactions and derive rate equations involved in cellulose deconstruction. The model reactions in this work are formulated based on the existing understanding of reaction mechanisms as outlined in the previous section. Two kinds of reactions taking place during cellulose deconstruction are (i) random scission of glycosidic bonds in a given cellulose chain giving rise to two new cellulose chains with a reduced degree of polymerization and (ii) end-chain scission of cellulose resulting in the formation of glucose and other cellulose-oligomers. Cellulose-oligomers considered in this work include cellobiose (dimer), cellotriose (trimer), cellotetraose (tetramer), cellopentaose (pentamer), and cellohexaose (hexamer). The two cleavage reactions of cellulose are written as follows, where $C(x,t)$ represents the time-dependent molecular weight distribution of cellulose and x represents the molecular weight.



Here $Q_s(x_s)$ represents glucose when $s = 1$ and other oligomers of cellulose when $s = 2, 3, 4, 5$, and 6 . The decomposition reactions of cellulose-oligomers are essentially end-chain scissions and are written as



Based on the above generalized reaction, nine different reactions of hydrolysis of oligomers are possible. The rate coefficients, k_r , k_c , and k_q , denote random and end-chain scissions. These coefficients are assumed to be independent of chain length of cellulose, as hydrolysis occurs by the attack of a proton unlike thermal reactions wherein covalent bond fission occurs by the initial heat energy supplied. As the mechanism of glucose degradation is complex, the simplified equation of the Saeman model¹⁴ was adopted, which is represented as follows.



The degradation products usually include 5-hydroxymethyl furfural, 1,6-anhydroglucose, levulinic acid, and formic acid.²³ As the concentration profiles of the above intermediates under dilute acid–high temperature and concentrated acid–low temperature regimes are not reported in a majority of the earlier works, we lumped the glucose degradation products. Moreover, the mechanism of formation of these intermediates is complex and is still being investigated.^{29,30}

Population balance equations (PBEs) for cellulose deconstruction by the two kinds of scissions and cellulose-oligomer and glucose degradation reactions occurring in a batch reactor can be written as

$$\begin{aligned} \frac{\partial c(x, t)}{\partial t} = & -k_r c(x, t) - (k_\alpha + k_\beta + 4k_\gamma) c(x, t) \\ & + 2k_r \int_x^\infty c(x', t) \Omega_r(x, x') dx' \\ & + k_\alpha \int_x^\infty c(x', t) \Omega_1(x' - x_1, x') dx' \\ & + k_\beta \int_x^\infty c(x', t) \Omega_2(x' - x_2, x') dx' \\ & + \left(\sum_{s=3}^6 k_\gamma \int_x^\infty c(x', t) \Omega_s(x' - x_s, x') dx' \right) \end{aligned} \quad (2)$$

$$\frac{\partial q_6}{\partial t} = k_\gamma \int_x^\infty c(x', t) \Omega_6(x_6, x') dx' - 3k_\delta q_6(x_6, t) \quad (3)$$

$$\begin{aligned} \frac{\partial q_5}{\partial t} = & k_\gamma \int_x^\infty c(x', t) \Omega_5(x_5, x') dx' + k_\delta q_6(x_6, t) \\ & - 2k_\delta q_5(x_5, t) \end{aligned} \quad (4)$$

$$\begin{aligned} \frac{\partial q_4}{\partial t} = & k_\gamma \int_x^\infty c(x', t) \Omega_4(x_4, x') dx' + k_\delta q_6(x_6, t) \\ & + k_\delta q_5(x_5, t) - 2k_\delta q_4(x_4, t) \end{aligned} \quad (5)$$

$$\begin{aligned} \frac{\partial q_3}{\partial t} = & k_\gamma \int_x^\infty c(x', t) \Omega_3(x_3, x') dx' + k_\delta q_6(x_6, t) \\ & + k_\delta q_5(x_5, t) + k_\delta q_4(x_4, t) - k_\delta q_3(x_3, t) \end{aligned} \quad (6)$$

$$\begin{aligned} \frac{\partial q_2}{\partial t} = & k_\beta \int_x^\infty c(x', t) \Omega_2(x_2, x') dx' + k_\delta q_6(x_6, t) \\ & + k_\delta q_5(x_5, t) + k_\delta q_4(x_4, t) + k_\delta q_3(x_3, t) \\ & - k_{\delta 1} q_2(x_2, t) \end{aligned} \quad (7)$$

$$\begin{aligned} \frac{\partial q_1}{\partial t} = & k_\alpha \int_x^\infty c(x', t) \Omega_1(x_1, x') dx' + k_\delta q_6(x_6, t) \\ & + k_\delta q_5(x_5, t) + k_\delta q_4(x_4, t) + k_\delta q_3(x_3, t) \\ & + k_{\delta 1} q_2(x_2, t) - k_g q_1(x_1, t) \end{aligned} \quad (8)$$

Here q_1, q_2, q_3, q_4, q_5 , and q_6 and x_1, x_2, x_3, x_4, x_5 , and x_6 represent concentrations and molecular weights of glucose, cellobiose, cellotriose, cellotetraose, cellopentaose, and cellohexaose, respectively. The rate coefficient k_r denotes cellulose deconstruction by random scission; k_α, k_β , and k_γ denote the formation of glucose, cellobiose, and other cellulose-oligomers, respectively, via end-chain scission; k_δ and $k_{\delta 1}$ denote glucose

production from cellulose-oligomers and cellobiose, respectively, and k_g denotes the degradation of glucose. Based on the type of scission, the stoichiometric kernels are given by^{31,32}

$$\text{Random chain scission: } \Omega_r(x, x') = 1/x' \quad (9)$$

$$\begin{aligned} \text{End-chain scission } \Omega_s(x' - x_s, x') &= \delta(x - (x' - x_s)), s \\ &= 1 - 6 \end{aligned} \quad (10)$$

$$\Omega_s(x_s, x') = \delta(x - x_s), s = 1 - 6 \quad (11)$$

Equation 9 signifies the distribution of cellulose chains owing to the scission of a glycosidic bond at any random position; eq 10 signifies the distribution of cellulose chains formed after unzipping of the oligomers, and eq 11 signifies the evolution of oligomers of fixed molecular weight x_s ($s = 1-6$). The PBEs were converted to ordinary differential equations (ODEs) using method of moments, wherein the n th order moment is defined as^{31,32}

$$c^{(n)} = \int_0^\infty x^n c(x, t) dx \quad (12)$$

The transformed rate equations are represented by eqs 13–19.

$$\begin{aligned} \frac{dc^{(n)}}{dt} &= -\left(\frac{n-1}{n+1}\right)k_r c^{(n)} - (k_{\alpha} c^{(n)} + k_{\beta} c^{(n)} + 4k_{\gamma} c^{(n)}) \\ &\quad + \sum_{j=0}^n \binom{n}{j} (k_{\alpha} x_1^j + k_{\beta} x_2^j + \sum_{s=3}^6 k_{\gamma} x_s^j) (-1)^j c^{(n-j)} \end{aligned} \quad (13)$$

$$\frac{dq_s^{(n)}}{dt} = k_{\gamma} x_s^n c^{(0)} + -3k_{\delta} x_6^n q_6^{(0)} \quad (14)$$

$$\frac{dq_5^{(n)}}{dt} = k_{\gamma} x_5^n c^{(0)} + k_{\delta} x_6^n q_6^{(0)} - 2k_{\delta} x_5^n q_5^{(0)} \quad (15)$$

$$\frac{dq_4^{(n)}}{dt} = k_{\gamma} x_4^n c^{(0)} + k_{\delta} x_6^n q_6^{(0)} + k_{\delta} x_5^n q_5^{(0)} - 2k_{\delta} x_4^n q_4^{(0)} \quad (16)$$

$$\begin{aligned} \frac{dq_3^{(n)}}{dt} &= k_{\gamma} x_3^n c^{(0)} + k_{\delta} x_6^n q_6^{(0)} + k_{\delta} x_5^n q_5^{(0)} + k_{\delta} x_4^n q_4^{(0)} \\ &\quad - k_{\delta} x_3^n q_3^{(0)} \end{aligned} \quad (17)$$

$$\begin{aligned} \frac{dq_2^{(n)}}{dt} &= k_{\beta} x_2^n c^{(0)} + k_{\delta} x_6^n q_6^{(0)} + k_{\delta} x_5^n q_5^{(0)} + k_{\delta} x_4^n q_4^{(0)} \\ &\quad + k_{\delta} x_3^n q_3^{(0)} - k_{\delta} x_2^n q_2^{(0)} \end{aligned} \quad (18)$$

$$\begin{aligned} \frac{dq_1^{(n)}}{dt} &= k_{\alpha} x_1^n c^{(0)} + k_{\delta} x_6^n q_6^{(0)} + k_{\delta} x_5^n q_5^{(0)} + k_{\delta} x_4^n q_4^{(0)} \\ &\quad + k_{\delta} x_3^n q_3^{(0)} + k_{\delta} x_2^n q_2^{(0)} - k_{\delta} x_1^n q_1^{(0)} \end{aligned} \quad (19)$$

The above ODEs were solved for zeroth ($n = 0$) and first ($n = 1$) order moments by setting the initial conditions to be $C^{(0)}(t = 0) = C_0$, $C^{(1)}(t = 0) = C_0 \times M_{n0}$, and $q_s^{(0)}(t = 0) = 0$ (for $s = 1-6$), where C_0 is the initial molar concentration of cellulose and M_{n0} is the initial number-average molecular weight of cellulose, to obtain the profiles of molar

concentration (mol/L) and mass concentration (g/L) of various species.

2.3. Model Details. On the basis of the discussion in the mechanism section, proton attack on glycosidic oxygen is treated as the dominant pathway of acid hydrolysis of cellulose.²⁶ Hence, all the reactions considered in the proposed mechanism are assumed to follow the dominant pathway, and all other side reactions, which are nonsignificant, are ignored. Pilath et al.³³ reported the formation of glucose from cellobiose to be nearly 100 times faster than the reverse reaction. Therefore, all the reactions involved in the acid hydrolysis model are treated to be irreversible, pseudo-first-order reactions. It is intuitive that the rate constants of hydrolysis reactions would differ under dilute and concentrated acid conditions, owing to the heterogeneous and homogeneous nature of the reactions, respectively. In this study the pre-exponential factors for the formation of cellotriose, cellotetraose, cellopentaose, and cellohexaose from cellulose and that for the formation of glucose from cellotriose, cellotetraose, cellopentaose, and cellohexaose were treated to be the same as the reported values fall in a comparable range.³⁴ This is reasonable as the effect of acid concentration on kinetics is incorporated via A^m in all the rate constant expressions. In other words, the product of the pre-exponential factor of a particular reaction type and A^m is different for dilute and concentrated acid regimes owing to different values of m under these conditions. Moreover, the rates of all possible reactions of cellotetraose, cellopentaose, and cellohexaose that lead to nonglucose oligomers were assumed to be the same as that of their reactions producing glucose. The dependence of reaction rate on acid concentration is incorporated as an independent parameter in the rate constant according to eq 1.¹⁴ Thus, k_r , k_{α} , k_{β} , k_{γ} , k_{δ} , and $k_{\delta 1}$ that signify the decomposition of cellulose and its oligomers to various products are dependent on acid exponent, m . The rate constant for glucose degradation, k_g , was assumed to be dependent on the acid exponent, n , and temperature exponent, y , according to the modified Arrhenius equation (eq 20) as stated by IUPAC.³⁵ This is justifiable based on the results of Mosier et al.,³⁶ who observed the rate of glucose degradation in the presence of sulfuric acid to be more sensitive to temperature than that in the presence of other organic acids.

$$k_g = k_{g0} A^n T^y \exp\left(\frac{-E_{ag}}{RT}\right) \quad (20)$$

Here k_{g0} is the pre-exponential factor, E_{ag} is the activation energy of glucose degradation, y is a measure of dependence of degradation reaction on temperature. As the initial molecular weight of cellulose is not reported in a majority of the experimental works, we have taken, for the sake of uniformity, the degree of polymerization of cellulose to be 847, which corresponds to a number-average molecular weight, M_n , of 135 554 g/mol and a polydispersity, PDI, of 2.25. This corresponds to microcrystalline cellulose produced by Sigma-Aldrich.³⁷

3. RESULTS AND DISCUSSION

Experimental batch reactor data for fitting and evaluation of model parameters was obtained from various earlier studies,^{11,13,15-17,38-40} corresponding to acid hydrolysis of pure cellulose such as α -cellulose, microcrystalline cellulose, and cellulose extracted from lignocellulosic biomasses such as paper refuse and sugar cane bagasse in the presence of sulfuric acid at

Table 2. Kinetic Parameters Utilized in the Unified Model of Cellulose Acid Hydrolysis

kinetic parameters	dilute acid and high temperature	concentrated acid and low temperature	ref
m	2.05 ± 0.01	2.59 ± 0.05	this work
n	3.13 ± 0.01	2.36 ± 0.02	this work
k_{a0} (min^{-1})	4.55×10^{17}	4.55×10^{17}	18
$k_{\beta 0}$ (min^{-1})	1.95×10^{16}	1.95×10^{16}	22
$k_{\gamma 0}$ (min^{-1})	4.8×10^{15}	4.8×10^{15}	13
$k_{\tau 0}$ (min^{-1})	6.06×10^{14}	6.06×10^{14}	41
E_a (kJ/mol)	134	134	42
$k_{\delta 0}$ (min^{-1})	6.99×10^{16}	6.99×10^{16}	34
$k_{\delta 10}$ (min^{-1})	5.906×10^{15}	5.906×10^{15}	34
$E_{a\delta}$ (kJ/mol), $E_{a\delta 1}$ (kJ/mol)	134	134	38
k_{g0} ($\text{min}^{-1}/\text{K}^y$) ^a	4×10^{10}	3×10^{10}	19
E_{ag} (kJ/mol)	137	137	38
E_{ar} (kJ/mol)	137	137	42
y	2.37 ± 0.02	2.40 ± 0.01	this work

^aThe product, $k_{g0}T^y$, matched well with Arrhenius k_{g0} reported by Abatzoglov et al.¹⁹

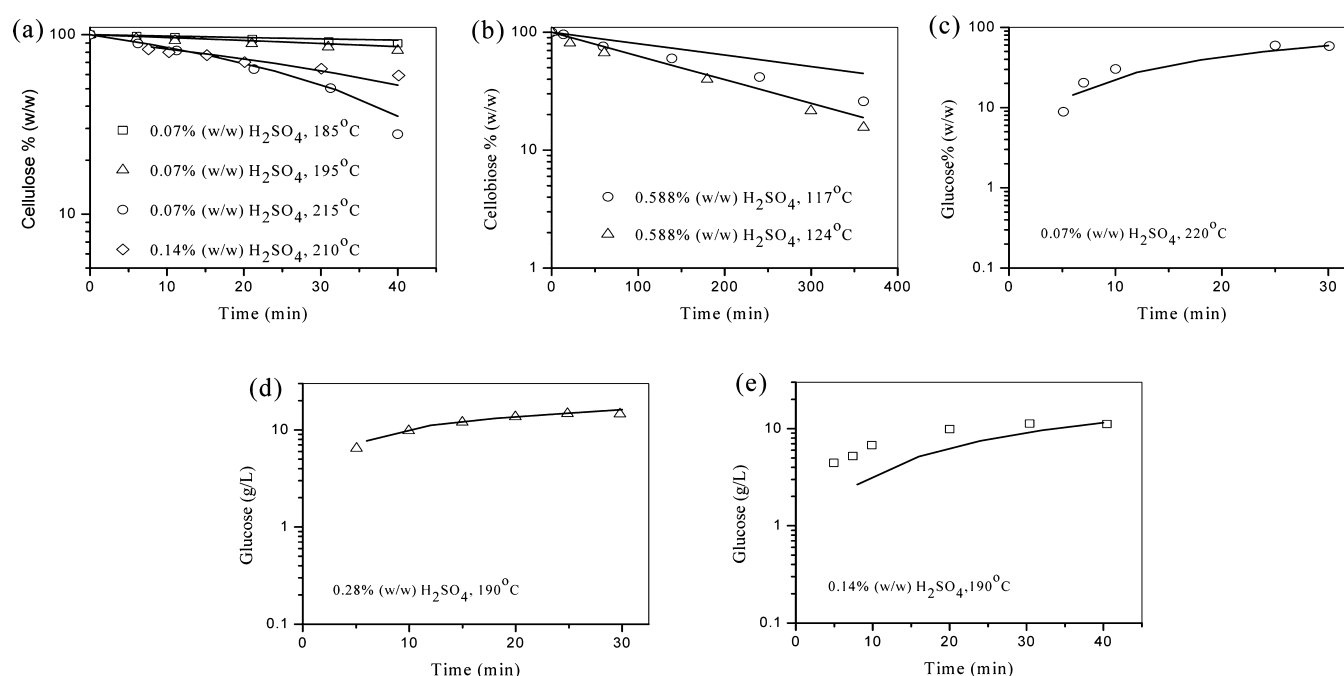


Figure 2. Curve-fitted plots for cellulose acid hydrolysis at dilute acid and high temperatures: (a) Effect of temperature and acid concentration on cellulose deconstruction (exptl. data: Gurgel et al.,¹³ Xiang et al.⁴⁰). (b) Influence of temperature on cellobiose hydrolysis (exptl. data: Dadach and Kaliaguine³⁸). (c, d, e) Effect of temperature and acid concentration on glucose production (exptl. data: Kim et al.,¹¹ Gurgel et al.¹³). Lines denote model profiles.

different concentrations. The ODEs given by eqs 13–19 for $n = 0$ and 1 for all the species at specific reaction conditions were solved using ODEsolver45 in MATLAB. The model was fitted with the experimental data using least-squares curvefit toolbox in MATLAB to determine the values of key parameters that influence cellulose deconstruction and glucose production at conditions ranging from extremely low (0.07%) to high (70%) acid concentrations and high (225 °C) to low (25 °C) temperatures. The rate kinetics were observed for two distinct regimes, namely, dilute acid hydrolysis at high temperatures and concentrated acid hydrolysis at low temperatures. Observations of acid concentration being the major factor affecting the rate of cellulose deconstruction, as reported in section 2.1, substantiate this classification. The degree of dependence of rate constants on the parameters stated above was investigated by fitting the acid exponents, m and n , and the temperature exponent, y , for

various reaction conditions, as discussed in the following subsections. All the kinetic parameters are summarized in Table 2.^{13,18,19,22,34,38,41,42} The pre-exponential factor for random chain scission, $k_{\tau 0}$, was chosen to be similar to that of pre-exponential factor reported for hydrolysis of crystalline cellulose using HCl, as the inner sites of cellulose are essentially crystalline in nature.⁴¹ The pre-exponential factor for glucose degradation was chosen such that the product, $k_{g0}T^y$, according to a modified Arrhenius equation was in agreement with the value of the Arrhenius pre-exponential factor reported by Abatzoglov et al.¹⁹ for a wide range of temperatures. Later, this model was also tested for acid hydrolysis of actual biomasses such as walnut green skin (WGS), paper refuse (PR), and yellow poplar wood (YPW).

3.1. Dilute Acid and High Temperature Conditions. Experimental data for cellulose and glucose hydrolysis have

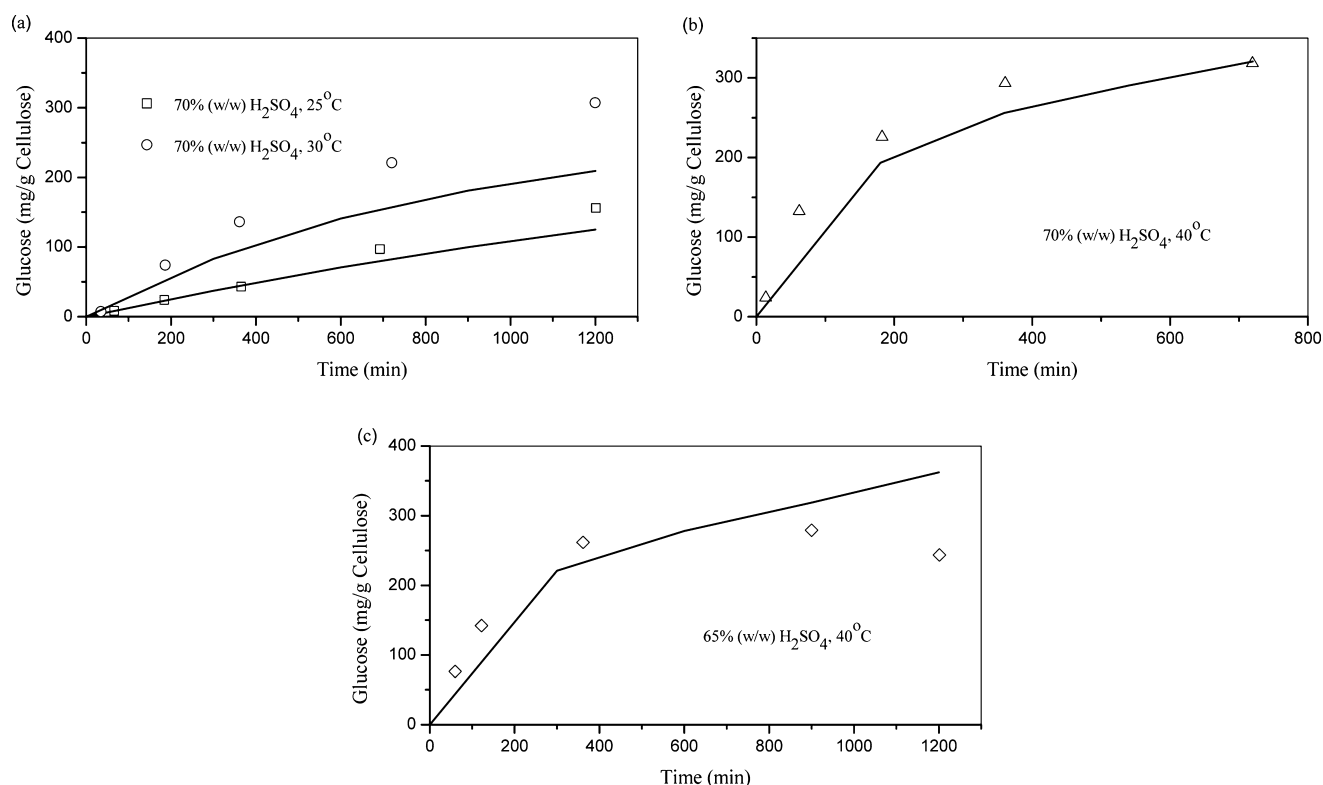


Figure 3. Curve-fitted plots for cellulose acid hydrolysis at concentrated acid and low temperatures: (a, b) Variation of glucose production with temperature, (c) effect of acid concentration on glucose production (exptl. data: Camacho et al.¹⁶). Lines denote model profiles.

been selectively chosen in the temperature range of 185–220 °C at 0.07%, 0.14%, and 0.28% (w/w) H_2SO_4 . Cellobiose hydrolysis at moderate temperatures (117 and 124 °C) was also grouped under the same category as the percentage of H_2SO_4 was falling under low acid conditions, i.e. 0.588% (w/w) H_2SO_4 . Figure 2a and b depict the plots for cellulose and cellobiose hydrolysis. Cellulose deconstruction profiles of the model satisfactorily matched the experimental data. Here, the effect of temperature was predominant on the conversion of cellulose. At temperatures lower than 200 °C, cellulose conversion was very low owing to a slow rate of reaction as explained in the theory of heterogeneous acid hydrolysis. The conversion increased very rapidly with an increase in temperature indicating solubilization of cellulose at higher temperatures allowing more hydrogen ion attack on cellulose. While an increase in H_2SO_4 concentration increased the conversion, the same can also be attributed to the effect of temperature. Thus, the acid concentration under such dilute conditions did not have a significant effect on cellulose conversion. In order to fit the experimental data of cellobiose hydrolysis, the model was reduced to two equations, namely, the formation of glucose from cellobiose and degradation of glucose using the corresponding rate parameters as shown in Table 2. The model profiles of cellobiose conversion matched well with experimental data at 124 °C, while at 117 °C there was a variation at long time periods greater than 200 min. However, the overall trends were well captured. This elucidates the robustness of the model in terms of its applicability for acid hydrolysis of cellulose as well as its oligomers. Importantly, the glucose yields were significantly affected both by temperature and acid concentration (Figures 2c, d, and e). At temperatures corresponding to 190 °C, the production of glucose was low due to low conversion of cellulose. However, the yield of

glucose was constant after 10 min owing to a higher rate of degradation of glucose induced by the acid, whose concentration was more than 0.14%, as shown in Figure 2d,e. At higher temperatures corresponding to 220 °C, the yield of glucose increased rapidly but ceased due to its degradation, in this case, due to the effect of temperature. The values of m , n , and y evaluated by least-squares curve fitting were 2.05 ± 0.01 , 3.13 ± 0.01 , and 2.37 ± 0.01 , respectively. The values m , n , and y indicate that the reaction rate of cellulose deconstruction increased by 2% for every 1% increase in acid concentration, and rate of glucose degradation increased by 3.2% and 2.4% for every 1% increase in acid concentration and temperature, respectively. Such a good agreement of the model with experimental data under dilute acid and high temperature concentrations supports the proposed mechanism of cellulose acid hydrolysis.

3.2. Concentrated Acid and Low Temperature Conditions. Experimental data of cellulose acid hydrolysis at high acid concentration was chosen in the temperature range of 25–40 °C at 65% and 70% (w/w) H_2SO_4 . At such high acid concentrations, cellulose is expected to solubilize in the liquid phase, and the nature of the reaction becomes homogeneous. Although the reactions are expected to occur at a much faster rate when compared to heterogeneous hydrolysis of cellulose, hydrolysis under homogeneous conditions occurs at a much slower rate as reflected in Figure 3. This is in good agreement with theory, according to which cellulose conversion to glucose or LMWPs will not be initiated unless the crystalline cellulose matrix is completely disrupted and dissolved in the acid, and hence, the reaction times are as high as 20 h. While a reasonable match of model glucose profiles with experimental data was observed, the trends of glucose evolution were well captured by the model. The values of m , n , and y obtained by least-squares

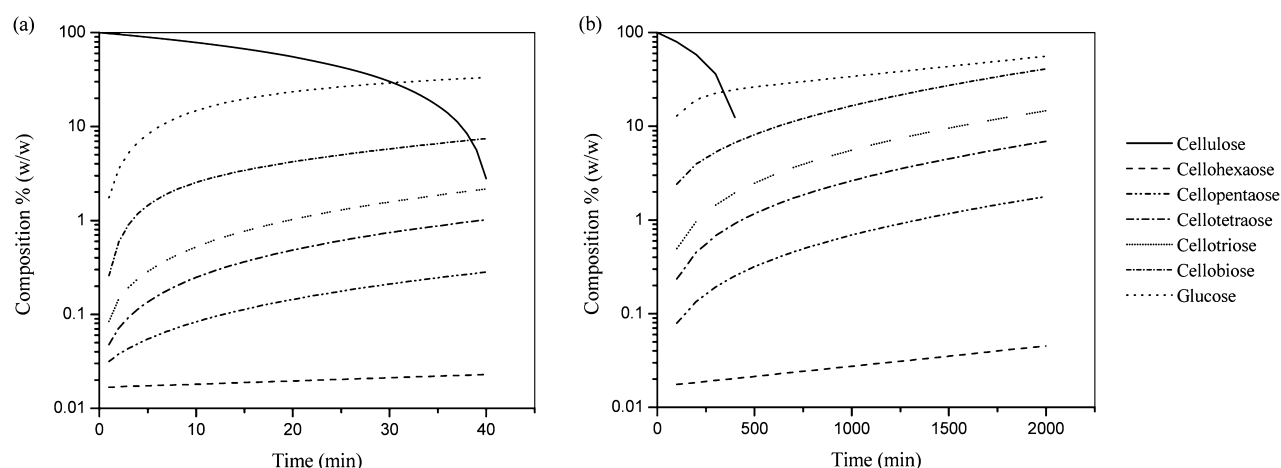


Figure 4. Model predictions of cellulose, cellulose-oligomers, and glucose profiles under various conditions: (a) 0.07 wt % of H_2SO_4 at 220 °C, (b) 70 wt % H_2SO_4 at 40 °C.

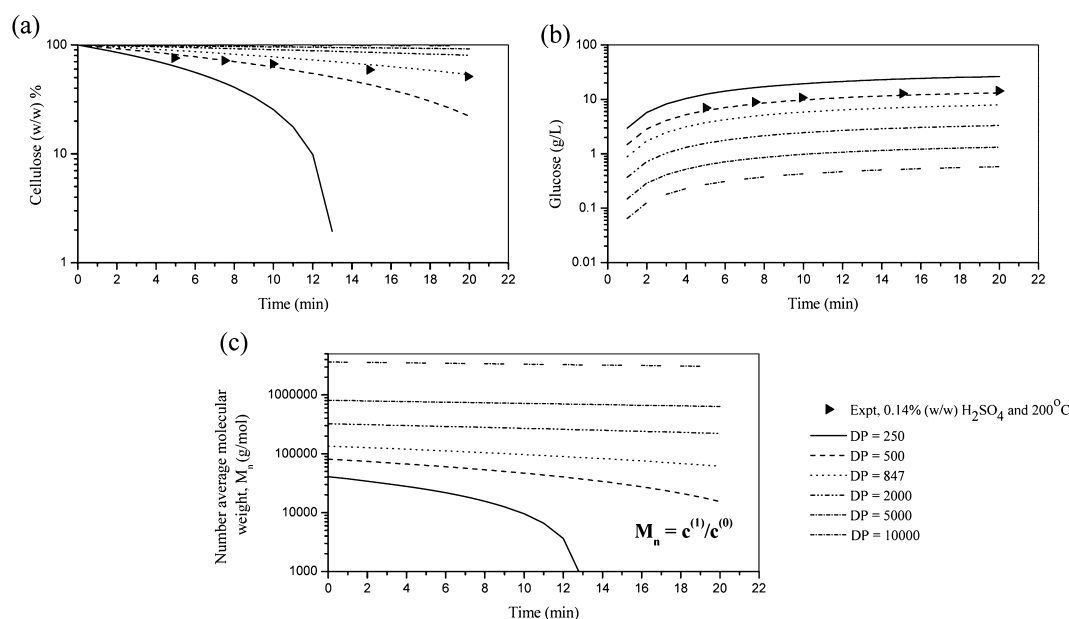


Figure 5. Effect of initial degree of polymerization (DP) on (a) cellulose conversion and (b) glucose yield, both at 0.14 wt % of H_2SO_4 and 200 °C. (c) Variation of number-average molecular weight ($c^{(1)}/c^{(0)}$) of cellulose with respect to time under the above-mentioned conditions (exptl. data: Gurgel et al.¹³).

fitting were 2.59 ± 0.05 , 2.37 ± 0.02 , and 2.4 ± 0.01 , respectively. Physical effects of these parameters are evident from the glucose profiles under concentrated acid conditions (Figure 3). At room temperatures of 25 and 30 °C, glucose production is sufficiently high, and linear indicating no or a very low rate of degradation reactions taking place at such low temperatures. A slight increase in temperature to 40 °C boosted the degradation reactions to occur at much faster rates, which is observed by the change of slope around 190 min (Figure 3b), justifying the combined effect of acid (n) and temperature exponents (y). Moreover, at room temperatures, the effect of H_2SO_4 concentration on the initial yield of glucose is less pronounced, while at 40 °C the initial rate of production of glucose is significantly higher, which is indicated by a much steeper slope in the initial period of hydrolysis (Figure 3a,b). A change in slope in Figure 3c at around 300 min indicates the shift in rate owing to degradation reactions, but since the H_2SO_4 concentration is slightly lesser than that of Figure 3b, it

is observed after a longer time. The above discussion also substantiates the sensitivity of glucose degradation reactions to acid concentration.

3.3. Model Predicted Profiles of Oligomers. A model simulation tracking the time evolution of all the intermediates was performed at 220 °C and 0.07% (w/w) H_2SO_4 . The simulation was run for 40 min, and the results are depicted in Figure 4a. The rate of cellulose deconstruction was higher due to very high temperature, and nearly complete conversion was observed within 40 min. The model predicted ratios of yields of cellobiose, cellotriose, cellotetraose, cellopentaose, and cellohexaose with respect to glucose were 0.2235, 0.0646, 0.03059, 0.0089, and 0.0007, respectively, while those evaluated using area under the chromatogram reported by Xiang et al.¹² were 0.1234, 0.068, 0.0302, 0.0195, and 0.0096. These results match reasonably well with experimental data and prove that the proposed model indeed captures the trends of the cellulose-oligomers in addition to the key product, glucose. Importantly,

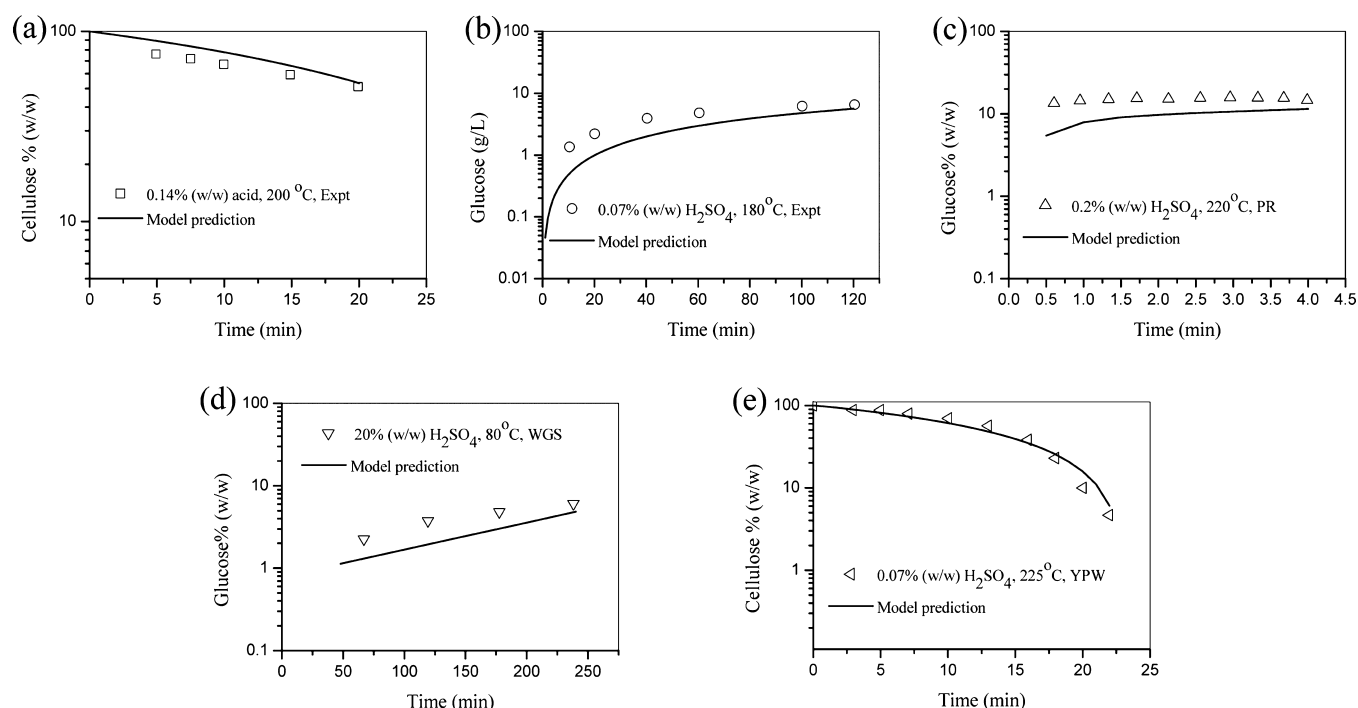


Figure 6. Validation of model predictions: (a, b) Cellulose and glucose profiles during acid hydrolysis of cellulosic pulp extracted from sugar cane bagasse (exptl. data: Gurgel et al.¹³). (c) Glucose profile according to isothermal model of acid hydrolysis of paper refuse (PR) (exptl. data: Fagan et al.¹⁷). (d) Glucose production from acid hydrolysis of walnut green skin (WGS) (exptl. data: Arastehnodeh et al.¹⁵). (e) Cellulose profile during hydrolysis of yellow poplar wood (YPW) (exptl. data: Torget et al.³⁹).

the concentration profiles of cellulo-oligomers are usually not reported in a majority of the existing studies, and our model will be useful to understand these trends at different reaction conditions. The profiles of oligomers and glucose increased continuously indicating reactions of solubilized cellulose fractions.

The reaction conditions for the simulation of concentrated acid–low temperature hydrolysis were chosen at 40 °C and 70% (w/w) H_2SO_4 . The time taken for cellulose to get completely converted was approximately 450 min, and the yield of glucose after a reaction time of 20 h was nearly 56% (Figure 4b). This indicates the possibility of solubilization of crystalline cellulose in solution thereby providing room for the smaller cellulose chains to bind in a more regular fashion, thus increasing its crystallinity and, hence, longer reaction times. Under such concentrated acid conditions, the model predicted ratios of oligomers with respect to glucose were 0.733, 0.262, 0.123, 0.0314, and 0.0008 for cellobiose, cellotriose, cellotetraose, cellopentaose, and cellohexaose, respectively, which are approximately 2.5 to 4 times that reported by Xiang et al.¹² for extremely dilute acid and high temperature conditions. This proves that the trends of cellulo-oligomer yields are in agreement with those found in the experiments. Interestingly, the yield of cellohexaose is nearly the same as that observed for dilute acid conditions. This indicates that the rate of formation of cellohexaose is very slow when compared to all other end scission products, which might be due to strong hindrance toward glycosidic bond cleavage induced by hydrogen bonding.

3.4. Effect of Initial Concentration and Degree of Polymerization of Cellulose. The effects of initial concentration and degree of polymerization, DP, of cellulose on the yield of glucose were examined for an acid concentration of 0.14% H_2SO_4 at 200 °C. It was observed that the initial mass concentration of cellulose, in a broad range of 10–100 g/L with

$M_n = 135\,554$ g/mol and PDI = 2.25, had no effect on final percent conversion of cellulose and yield of glucose. Although, in reality, various transport effects creep while handling such large amounts of solids (100 g/L), these were neglected as this study focuses primarily on the reaction kinetics of cellulose deconstruction. However, the initial molecular weight of cellulose had a significant effect on percent conversion of cellulose and yield of glucose (Figure 5a,b). The DP of model cellulosic substrates like Avicel, cotton, filter paper, bacterial cellulose, phosphoric acid swollen cellulose, and cellulose extracted from wood pulp varies in the range of 100 to 3000, while that of natural cotton is as high as 15 000.⁴³ Therefore, a range of initial DPs from 250 to 10 000 was chosen to understand its effect on cellulose conversion and glucose yields.⁴³ Hydrolysis of low molecular weight cellulose with a DP of 250 was much faster than that of high molecular weight cellulose with a DP of 10 000. This is expected as intermolecular, interchain, and intersheet hydrogen bonding in cellulose, and hence its crystallinity, are more pronounced in cellulose with longer chains compared to shorter ones. These predictions were validated with experimental cellulose and glucose profiles reported by Gurgel et al.¹³ The experimental profile of cellulose conversion was observed to be in between the model predictions corresponding to DP of 500 and 847, whereas the model prediction corresponding to a DP of 500 matches well with the experimental glucose profile. The variation of number-average molecular weight, M_n , calculated as the ratio of mass to molar concentration of cellulose, $c^{(1)}/c^{(0)}$, with time under the same reaction condition for various initial DP of cellulose is depicted in Figure 5c. It is important to note that the variation of M_n with time is similar to that of cellulose conversion. For a very low DP of 250, there is a drastic reduction in molecular weight after 10 min which is quite similar to the trend observed for cellulose conversion. The

above observations demonstrate that cellulose conversion and glucose yield largely depend on the initial crystallinity of cellulose, which in this work is quantified in terms of degree of polymerization. This shows that the initial molecular weight of cellulose is an important factor to be considered in acid hydrolysis experiments as it is directly related to cellulose conversion and glucose yields.

3.5. Model Validation and Insights. The validity of the model was evaluated for experimental data of cellulose hydrolysis for various reaction conditions (Figure 6a and b). The model was also validated with the predictions of the Saeman model for hydrolysis of paper refuse¹⁷ (Figure 6c). It is evident that the model predictions are in good agreement with experiments under all types of reaction conditions. The model was also validated with experimental data of acid hydrolysis of two biomasses, namely walnut green skin (WGS)¹⁵ and yellow poplar wood (YPW),³⁹ by utilizing the parameters m , n , and y within the uncertainty limits corresponding to concentrated acid–low temperature for WGS and dilute acid–high temperature for YPW. It is clear that the model predicted cellulose profile for YPW hydrolysis matches well with the experimental data while the model predicted glucose profile for WGS hydrolysis captures the experimental trend, albeit with a variation in the initial time period up to 150 min. It is important to note that the mechanism of acid hydrolysis of whole biomass is not as straightforward as acid hydrolysis of cellulose, owing to the presence of hemicelluloses, lignin, ash, and other extractives in varying proportions. These materials tend to inhibit the solubilization of cellulose and, hence, decrease the rate of production of sugars. This can occur either by the formation of complexes of hemicellulose, lignin, ash, and other extractives with cellulose and oligomers to form new byproducts or by the competition of dominant cellulose deconstruction pathways with that of other biomass components. Interestingly, YPW contains 41.9% cellulose, 23.5% hemicelluloses, 26.6% lignin, 3.4% acetyl intermediates, and only 0.6% ash,³⁹ while WGS contains only 21.5% cellulose, 13.25% hemicelluloses, 18.25% extractives, 26.07% lignin, and 20.93% ash.¹⁵ Thus, the better match of the model predicted cellulose profile with the experimental data of YPW hydrolysis can be attributed to the high content of cellulose and low content of ash in YPW, while the low content of cellulose and high content of ash and extractives in WGS leads to variations between model prediction and experimental data for WGS acid hydrolysis. Moreover, the effect of parameters n and y for dilute-acid hydrolysis of yellow poplar wood at 225 °C and 0.07% (w/w) H_2SO_4 were found to be the same as that in cellulose hydrolysis. However, there was an increase in cellulose conversion by 1.96% for every 1% increase in H_2SO_4 concentration. Even though the effects of ash, extractives, and lignin are not incorporated in the model, the model still predicts the trends qualitatively, which proves that the model can be upgraded easily to incorporate the above effects.

An ensemble of the above observations shows that condensing the values of rate parameters for acid hydrolysis under the two regimes, namely, dilute acid–high temperature and concentrated acid–low temperature, is a promising approach to obtain an understanding of time evolution of cellulose, glucose, and oligomer profiles. The mechanistic kinetic model developed in this work predicted all possible phenomena that could occur during cellulose acid hydrolysis at various conditions utilizing a single set of rate parameters of the elementary steps. This is considerable when compared to the

existing understanding, which is based on utilizing different rate parameters for different reaction conditions as shown in Table 1. Importantly, the proposed model is validated with experimental data of acid hydrolysis of cellulose from different biomasses reported by various research groups.

4. CONCLUSIONS

In this work, a unified kinetic model for cellulose acid hydrolysis was developed by evaluating the kinetic parameters that determine the effects of acid and temperature on the formation of cellulo-oligomers and their subsequent reactions, apart from glucose formation and degradation reactions, for two widely different hydrolysis regimes. To the best of our knowledge, this is the first work to report a detailed mechanism of cellulose acid hydrolysis including random chain and end-chain scissions along with the reactions leading to the formation of cellulo-oligomers. A modified Arrhenius equation with additional temperature dependence was incorporated to account for the sensitivity of the reaction with respect to temperature in the presence of sulfuric acid. The dependence of rate constants on acid concentration and temperature under dilute and concentrated acid conditions was found by fitting the model with the experimental data. Values of acid and temperature exponents, m , n , and y , under dilute acid–high temperatures were 2.05 ± 0.01 , 3.13 ± 0.01 , and 2.37 ± 0.01 , respectively, while under concentrated acid–low temperature conditions were 2.59 ± 0.05 , 2.37 ± 0.02 , and 2.41 ± 0.01 , respectively. The trend observed in these parameters elucidates the role of acid concentration and temperature on the elementary reactions of acid hydrolysis. Under concentrated acid conditions, the acid completely solubilizes cellulose and thus makes glycosidic linkages more susceptible to acid attack. A high value of m , in this case, indicates the pronounced effect of acid on cellulose deconstruction. Similarly, under dilute conditions, a high value of n indicates that glucose molecules degrade more quickly with even a slight change in acid concentration. However, values of y remain nearly the same under dilute and concentrated conditions. From this, it can be concluded that temperature has similar effects under any reaction condition, but the concentration of acid determines the kinetics of cellulose deconstruction by controlling the possible physical effects underlying the mechanism of hydrolysis. Moreover, the effect of acid was more pronounced on the degradation of glucose, which is, interestingly, in sharp contrast with the pronounced effect of temperature on the degradation of xylose during acid hydrolysis of hemicellulose.⁴⁴ There was no effect of initial mass concentration of cellulose on its conversion and glucose yield, while the initial DP of cellulose significantly affected cellulose conversion and glucose yields. A high initial DP of cellulose leads to a high degree of hydrogen bonding between glycosidic oxygen and hydroxyl groups, thus increasing the crystallinity of cellulose. Hence low cellulose conversion and glucose production were observed. The model results also match well with the composition of the cellulo-oligomers in the hydrolysate reported by Xiang et al.¹² for hydrolysis of cellulose under dilute acid conditions. Hence, our model will be useful in understanding the trends of oligomers and glucose production under various reaction conditions, as these are not available in the existing studies. We also demonstrated the versatility of the model in a variety of reaction conditions and extended its applicability by validating the model predictions with acid hydrolysis data of

lignocellulosic biomasses like yellow poplar wood and walnut green skin.

AUTHOR INFORMATION

Corresponding Author

*Tel.: +91-44-2257 4187. E-mail: vinu@iitm.ac.in.

Notes

The authors declare no competing financial interest.

ACKNOWLEDGMENTS

R.V. thanks Department of Science and Technology (DST), India, for funding, and Indian Institute of Technology Madras for new faculty seed grant. The National Center for Combustion Research and Development is sponsored by DST, India. The authors thank the anonymous reviewers for constructive suggestions.

REFERENCES

- (1) Alvira, P.; Tomás-Pejó, E.; Ballesteros, M.; Negro, M. J. Pretreatment Technologies for an Efficient Bioethanol Production Process Based on Enzymatic Hydrolysis: A Review. *Bioresour. Technol.* **2010**, *101*, 4851.
- (2) Balat, M.; Balat, H.; Öz, C. Progress in Bioethanol Processing. *Prog. Energy Combust. Sci.* **2008**, *34*, 551.
- (3) Zheng, Y.; Pan, Z.; Zhang, R. Overview of Biomass Pretreatment for Cellulosic Ethanol Production. *Int. J. Agric. Biol. Eng.* **2009**, *2*, 51.
- (4) Chundawat, S. P. S.; Beckham, G. T.; Himmel, M. E.; Dale, B. E. Deconstruction of Lignocellulosic Biomass to Fuels and Chemicals. *Annu. Rev. Chem. Biomol. Eng.* **2011**, *2*, 121.
- (5) Agbor, V. B.; Cicek, N.; Sparling, R.; Berlin, A.; Levin, D. B. Biomass Pretreatment: Fundamentals toward Application. *Biotechnol. Adv.* **2011**, *29*, 675.
- (6) Pu, Y.; Hu, F.; Huang, F.; Davison, B. H.; Ragauskas, A. J. Assessing the Molecular Structure Basis for Biomass Recalcitrance during Dilute Acid and Hydrothermal Pretreatments. *Biotechnol. Biofuels* **2013**, *6*, 1.
- (7) Chundawat, S. P. S.; Balan, V.; Sousa, L. C.; Dale, B. E. Thermochemical Pretreatment of Lignocellulosic Biomass. In *Bioalcohol production: biochemical conversion of lignocellulosic biomass*; Waldron, K. W., Ed.; Woodhead Publishing: Sawston, Cambridge, U. K., 2010; pp 24–72.
- (8) Harmsen, P.; Huijgen, W.; Bermudez, L.; Bakker, R. *Literature Review of Physical and Chemical Pretreatment Processes for Lignocellulosic Biomass*; Wageningen UR, Food and Biobased Research: Wageningen, The Netherlands, 2010.
- (9) Taherzadeh, M. J.; Karimi, K. Pretreatment of Lignocellulosic Wastes to Improve Ethanol and Biogas Production: A Review. *Int. J. Mol. Sci.* **2008**, *9*, 1621.
- (10) Wyman, C. E.; Decker, S. R.; Himmel, M. E.; Brady, J. W.; Skopec, C. E. Hydrolysis of Cellulose and Hemicellulose. *Polysaccharides: Structural Diversity and Functional Versatility*; CRC Press: Boca Raton, FL, 2005; pp 1023–1062.
- (11) Kim, J.; Lee, Y. Y.; Torget, R. Cellulose Hydrolysis under Extremely Low Sulfuric Acid and High-Temperature Conditions. *Appl. Biochem. Biotechnol.* **2001**, *91–93*, 331.
- (12) Xiang, Q.; Kim, J.; Lee, Y. Y. A Comprehensive Kinetic Model for Dilute-Acid Hydrolysis of Cellulose. *Appl. Biochem. Biotechnol.* **2003**, *106*, 337.
- (13) Gurgel, L. V. A.; Marabezi, K.; Zambom, M. D.; Curvelo, A. A. S. Dilute Acid Hydrolysis of Sugar Cane Bagasse at High Temperatures: A Kinetic Study of Cellulose Saccharification and Glucose Decomposition. Part I: Sulfuric Acid as the Catalyst. *Ind. Eng. Chem. Res.* **2012**, *51*, 1173.
- (14) Saeman, J. F. Kinetics of Wood Saccharification-Hydrolysis of Cellulose and Decomposition of Sugars in Dilute Acid at High Temperature. *Ind. Eng. Chem.* **1945**, *37*, 43.
- (15) Arastehnodeh, A.; Ardjmand, M.; Fanaei, M. A.; Safekordi, A. A. Kinetic Modeling of Concentrated Acid Hydrolysis of Walnut Green Skin. *Afr. J. Biotechnol.* **2012**, *11*, 878.
- (16) Camacho, F.; Gonzalez-Tello, P.; Jurado, E.; Robles, A. Microcrystalline-Cellulose Hydrolysis with Concentrated Sulphuric Acid. *J. Chem. Technol. Biotechnol.* **1996**, *67*, 350.
- (17) Fagan, R. D.; Grethlein, H. E.; Converse, A. O.; Porteous, A. Kinetics of the Acid Hydrolysis of Cellulose Found in Paper Refuse. *Environ. Sci. Technol.* **1971**, *5*, 545.
- (18) Malester, I. A.; Green, M.; Shelef, G. Kinetics of Dilute Acid Hydrolysis of Cellulose Originating from Municipal Solid Wastes. *Ind. Eng. Chem. Res.* **1992**, *31*, 1998.
- (19) Abatzoglou, N.; Bouchard, J.; Chornet, E.; Overend, R. P. Dilute Acid Depolymerization of Cellulose in Aqueous Phase: Experimental Evidence of the Significant Presence of Soluble Oligomeric Intermediates. *Can. J. Chem. Eng.* **1986**, *64*, 781.
- (20) Thompson, D. R.; Grethlein, H. E. Design and Evaluation of a Plug Flow Reactor for Acid Hydrolysis of Cellulose. *Ind. Eng. Chem. Prod. Res. Dev.* **1979**, *18*, 166.
- (21) Franzidis, J.-P.; Porteous, A.; Anderson, J. The Acid Hydrolysis of Cellulose in Refuse in a Continuous Reactor. *Conserv. Recycl.* **1982**, *5*, 215.
- (22) Song, S. K.; Lee, Y. Y. Acid Hydrolysis of Wood Cellulose under Low Water Condition. *Biomass* **1984**, *6*, 93.
- (23) Conner, A. H.; Wood, B. F.; Hill, C. G., Jr.; Harris, J. F. Kinetic Model for the Dilute Sulfuric Acid Saccharification of Lignocellulose. *J. Wood Chem. Technol.* **1985**, *5*, 461.
- (24) Mok, W. S.; Antal, M. J., Jr.; Varhegyi, G. Productive and Parasitic Pathways in Dilute Acid-Catalyzed Hydrolysis of Cellulose. *Ind. Eng. Chem. Res.* **1992**, *31*, 94.
- (25) Xiang, Q.; Lee, Y. Y.; Torget, R. W. Kinetics of Glucose Decomposition during Dilute-Acid Hydrolysis of Lignocellulosic Biomass. *Appl. Biochem. Biotechnol.* **2004**, *113–116*, 1127.
- (26) Fengel, D.; Wegener, G. *Wood: Chemistry, Ultrastructure, Reactions*; de Gruyter: Berlin, 1983.
- (27) Soltes, E. J. *Wood as Agricultural Residues: Research on Use For Feed, Fuels, and Chemicals*; Soltes, E. J., Ed.; American Press: New York, 1983.
- (28) Dumitriu, S. *Polysaccharides: Structural Diversity and Functional Versatility*; CRC Press: Boca Raton, FL, 2005.
- (29) Qian, X.; Nimlos, M. R.; Davis, M.; Johnson, D. K.; Himmel, M. E. Ab Initio Molecular Dynamics Simulations of β -D-Glucose and β -D-Xylose Degradation Mechanisms in Acidic Aqueous Solution. *Carbohydr. Res.* **2005**, *340*, 2319.
- (30) Assary, R. S.; Curtiss, L. A. Comparison of Sugar Molecule Decomposition through Glucose and Fructose: A High-Level Quantum Chemical Study. *Energy Fuels* **2012**, *26*, 1344.
- (31) Kodera, Y.; McCoy, B. J. Distribution Kinetics of Radical Mechanisms: Reversible Polymer Decomposition. *AIChE J.* **1997**, *43*, 3205.
- (32) Madras, G.; Smith, J. M.; McCoy, B. J. Thermal Degradation Kinetics of Polystyrene in Solution. *Polym. Degrad. Stab.* **1997**, *58*, 131.
- (33) Pilath, H. M.; Nimlos, M. R.; Mittal, A.; Himmel, M. E.; Johnson, D. K. Glucose Reversion Reaction Kinetics. *J. Agric. Food Chem.* **2010**, *58*, 6131.
- (34) Freudenberg, K.; Blomqvist, G. Die Hydrolyse Der Cellulose Und Ihrer Oligosaccharide. *Ber. Dtsch. Chem. Ges.* **1935**, *68*, 2070.
- (35) Wilkinson, A. D.; McNaught, A. *IUPAC. Compendium of Chemical Terminology*, 2nd ed.; Blackwell Scientific Publications: Oxford, 1997; Vol. 68.
- (36) Mosier, N. S.; Ladisch, C. M.; Ladisch, M. R. Characterization of Acid Catalytic Domains for Cellulose Hydrolysis and Glucose Degradation. *Biotechnol. Bioeng.* **2002**, *79*, 610.
- (37) Vinu, R.; Broadbelt, L. J. A Mechanistic Model of Fast Pyrolysis of Glucose-Based Carbohydrates to Predict Bio-Oil Composition. *Energy Environ. Sci.* **2012**, *5*, 9808.
- (38) Dadach, Z.; Kaliaguine, S. Acid Hydrolysis of Cellulose. Part I. Experimental Kinetic Analysis. *Can. J. Chem. Eng.* **1993**, *71*, 880.

- (39) Torget, R. W.; Kim, J. S.; Lee, Y. Y. Fundamental Aspects of Dilute Acid Hydrolysis/fractionation Kinetics of Hardwood Carbohydrates. 1. Cellulose Hydrolysis. *Ind. Eng. Chem. Res.* **2000**, 39, 2817.
- (40) Xiang, Q.; Lee, Y. Y.; Pettersson, P. O.; Torget, R. W. Heterogeneous Aspects of Acid Hydrolysis of α -Cellulose. *Appl. Biochem. Biotechnol.* **2003**, 105 –108, 505.
- (41) Sidiras, D. K.; Koukios, E. G. Acid Saccharification of Ball-Milled Straw. *Biomass* **1989**, 19, 289.
- (42) Nelson, M. L. Apparent Activation Energy of Hydrolysis of Some Cellulosic Materials. *J. Polym. Sci.* **1960**, 43, 351.
- (43) Zhang, Y.-H. P.; Lynd, L. R. Toward an Aggregated Understanding of Enzymatic Hydrolysis of Cellulose: Noncomplexed Cellulase Systems. *Biotechnol. Bioeng.* **2004**, 88, 797.
- (44) Aguilar, R.; Ramírez, J. A.; Garrote, G.; Vázquez, M. Kinetic Study of the Acid Hydrolysis of Sugar Cane Bagasse. *J. Food Eng.* **2002**, 55, 309.